

# Dynamic loading leads to increased metabolic activity and spatial redistribution of viable cell density in nucleus pulposus tissue

**Citation for published version (APA):**

Salzer, E., Mouser, V. H. M., Bultink, J. A., Tryfonidou, M. A., & Ito, K. (2023). Dynamic loading leads to increased metabolic activity and spatial redistribution of viable cell density in nucleus pulposus tissue. *JOR Spine*, 6(1), Article e1240. <https://doi.org/10.1002/jsp2.1240>

**Document license:**  
CC BY-NC

**DOI:**  
[10.1002/jsp2.1240](https://doi.org/10.1002/jsp2.1240)

**Document status and date:**  
Published: 01/03/2023

**Document Version:**  
Publisher's PDF, also known as Version of Record (includes final page, issue and volume numbers)

**Please check the document version of this publication:**

- A submitted manuscript is the version of the article upon submission and before peer-review. There can be important differences between the submitted version and the official published version of record. People interested in the research are advised to contact the author for the final version of the publication, or visit the DOI to the publisher's website.
- The final author version and the galley proof are versions of the publication after peer review.
- The final published version features the final layout of the paper including the volume, issue and page numbers.

[Link to publication](#)

**General rights**

Copyright and moral rights for the publications made accessible in the public portal are retained by the authors and/or other copyright owners and it is a condition of accessing publications that users recognise and abide by the legal requirements associated with these rights.

- Users may download and print one copy of any publication from the public portal for the purpose of private study or research.
- You may not further distribute the material or use it for any profit-making activity or commercial gain
- You may freely distribute the URL identifying the publication in the public portal.

If the publication is distributed under the terms of Article 25fa of the Dutch Copyright Act, indicated by the "Taverne" license above, please follow below link for the End User Agreement:

[www.tue.nl/taverne](http://www.tue.nl/taverne)

**Take down policy**

If you believe that this document breaches copyright please contact us at:

[openaccess@tue.nl](mailto:openaccess@tue.nl)

providing details and we will investigate your claim.

## RESEARCH ARTICLE



# Dynamic loading leads to increased metabolic activity and spatial redistribution of viable cell density in nucleus pulposus tissue

Elias Salzer<sup>1</sup> | Vivian H. M. Mouser<sup>1</sup> | Jurgen A. Bulsink<sup>1</sup> |  
Marianna A. Tryfonidou<sup>2</sup> | Keita Ito<sup>1,3</sup>

<sup>1</sup>Orthopaedic Biomechanics, Department of Biomedical Engineering, Eindhoven University of Technology, Eindhoven, The Netherlands

<sup>2</sup>Department of Clinical Sciences, Faculty of Veterinary Medicine, Utrecht University, Utrecht, The Netherlands

<sup>3</sup>Institute for Complex Molecular Systems, Eindhoven University of Technology, Eindhoven, The Netherlands

## Correspondence

Keita Ito, Orthopaedic Biomechanics, Department of Biomedical Engineering, Eindhoven University of Technology, Eindhoven, The Netherlands.  
Email: [k.ito@tue.nl](mailto:k.ito@tue.nl)

## Funding information

Dutch Arthritis Society, Grant/Award Number: LLP22; H2020 European Research Council, Grant/Award Number: 825925

## Abstract

**Background:** Nucleus pulposus (NP) cell density is orchestrated by an interplay between nutrient supply and metabolite accumulation. Physiological loading is essential for tissue homeostasis. However, dynamic loading is also believed to increase metabolic activity and could thereby interfere with cell density regulation and regenerative strategies. The aim of this study was to determine whether dynamic loading could reduce the NP cell density by interacting with its energy metabolism.

**Methods:** Bovine NP explants were cultured in a novel NP bioreactor with and without dynamic loading in milieus mimicking the pathophysiological or physiological NP environment. The extracellular content was evaluated biochemically and by Alcian Blue staining. Metabolic activity was determined by measuring glucose and lactate in tissue and medium supernatants. A lactate-dehydrogenase staining was performed to determine the viable cell density (VCD) in the peripheral and core regions of the NP.

**Results:** The histological appearance and tissue composition of NP explants did not change in any of the groups. Glucose levels in the tissue reached critical values for cell survival ( $\leq 0.5$  mM) in all groups. Lactate released into the medium was increased in the dynamically loaded compared to the unloaded groups. While the VCD was unchanged on Day 2 in all regions, it was significantly reduced in the dynamically loaded groups on Day 7 ( $p \leq 0.01$ ) in the NP core, which led to a gradient formation of VCD in the group with degenerated NP milieu and dynamic loading ( $p \leq 0.05$ ).

**Conclusion:** It was demonstrated that dynamic loading in a nutrient deprived environment similar to that during IVD degeneration can increase cell metabolism to the extent that it was associated with changes in cell viability leading to a new equilibrium in the NP core. This should be considered for cell injections and therapies that lead to cell proliferation for treatment of IVD degeneration.

## KEYWORDS

ex vivo, glucose, intervertebral disc, mechanobiology, metabolism, nutrition

This is an open access article under the terms of the [Creative Commons Attribution-NonCommercial](https://creativecommons.org/licenses/by-nc/4.0/) License, which permits use, distribution and reproduction in any medium, provided the original work is properly cited and is not used for commercial purposes.

© 2022 The Authors. *JOR Spine* published by Wiley Periodicals LLC on behalf of Orthopaedic Research Society.

## 1 | INTRODUCTION

Back pain is a worldwide health problem and intervertebral disc degeneration (IVDD) is frequently associated with it.<sup>1</sup> Cells are dependent on nutrients and waste removal to survive and function properly. However, the cells in the IVD experience harsh conditions, especially in the central nucleus pulposus (NP). The IVD is the largest avascular organ in the human body, the nearest blood vessels to the NP core being up to 8 mm away in human lumbar IVDs.<sup>2</sup> Vital nutrients and toxic metabolites are transported to and from the NP cells residing within the core of the tissue mainly through the cartilaginous endplates.<sup>3,4</sup> While larger molecules can be transported via convective transport,<sup>5</sup> potentially due to the fluid flow during a diurnal cycle,<sup>6,7</sup> small molecules, such as glucose, lactate, and O<sub>2</sub>, are transported almost exclusively via diffusion.<sup>2</sup> Therefore, a potential onset of IVDD has been hypothesized to be due to disturbed molecular transport in the disc,<sup>2,8</sup> as for example the permeability of endplates decreases during IVDD.<sup>9</sup>

Associated with this limited nutrient environment, cell density is low in the NP, with only around 2–4 million cells/ml<sup>10,11</sup> and with increasing disc size, the cell density decreases.<sup>2</sup> During IVDD, when the cells' microenvironment changes from just sufficient to deprived nutrition, cells adapt to the new conditions with an altered cell density. Spatially, this means that regions closer to the blood supply have higher densities than regions further away, where glucose demand exceeds supply.<sup>2</sup> In IVD organ culture under limited nutrition conditions, a new equilibrium of cell viability was reached within days.<sup>12</sup>

The cells of the IVD adapt their energy metabolism to their microenvironment. Glucose consumption is dependent on cell density<sup>13</sup> and NP cells obtain their energy mainly via glycolysis, even in the presence of ambient oxygen conditions.<sup>3,14</sup> The metabolite lactate is extruded from cells and causes a decrease in the pericellular matrix pH.<sup>15–17</sup> This creates an imbalance of nutrient supply and waste removal that is hypothesized to lead to gradient formation where the resident NP cells experience the harshest conditions in the core of the tissue.<sup>8</sup> Nutrient/metabolite gradients cause metabolic rates of cells to be dependent on location in the disc.<sup>18</sup> Especially in the NP core, nutrient and metabolite turnover are low and critical levels for cell survival can be reached for the glucose concentration ( $\leq 0.5$  mM) and pH ( $\leq 6.7$ ) which supports only a limited cell density.<sup>13,14,19–21</sup> Interestingly, NP cells can survive for at least 12 days without oxygen<sup>13,14</sup> and hypoxia does not further decrease glucose or pH induced cell death.<sup>19</sup> It is therefore hypothesized, that an interplay of low glucose and low pH orchestrates cellular survival, as cell survival has been reported to be pH dependent at glucose levels between 0 and 0.5 mM, indicating a synergistic effect of glucose and pH for cell survival.<sup>2,19</sup>

Dynamic compression can increase metabolism of NP cells.<sup>22</sup> Therefore, it has been hypothesized that increased metabolic activity due to loading could reduce cell density<sup>2</sup> in a nutrient deprived environment, which could occur when attempting to regenerate the NP. However, it has not been determined if these changes in (energy) metabolism are sufficiently large enough to interact with the nutrient/

metabolite homeostasis in the NP and thus can affect cell survival. Therefore, the aim of this study was to determine if dynamic loading leads to an increased cellular metabolic activity in the NP under a nutrient deprived environment and whether the cell viability in the NP core would be affected. This was investigated in a bovine NP explant culture platform.

## 2 | MATERIALS AND METHODS

Bovine coccygeal NP explants were cultured for up to 7 days in a chemically and mechanically controlled environment. If not stated otherwise, chemicals were purchased from Sigma Aldrich (Zwijndrecht, the Netherlands).

### 2.1 | Nucleus pulposus explant culture

Bovine tails from 2 to 3 year-old cows were purchased from a slaughterhouse in accordance with local regulations. NP explants were aseptically prepared as previously described<sup>6</sup> from the first 4–5 intact proximal discs with a 8 mm biopsy punch (4–6 mm height). The different disc levels were distributed equally and randomly among the groups. The NP explants were cultured in a previously developed volume controllable NP culture chamber<sup>6,23</sup> (Figure 1A). To mimic the boundary conditions of the NP, that is, that of the inner annulus fibrosus, [glucose], oxygen tension and pH were adjusted to previously reported values in healthy and degenerated discs.<sup>3,14,17,24–29</sup> Culture medium (Table S1) consisted of Dulbecco's Modified Eagle Medium mimicking either the degenerative milieu (DM, i.e., 1 mM glucose, pH 6.8) or healthy milieu (HM, i.e., 3 mM glucose, pH 7.1) with 3% fetal bovine serum (Table 1). Explants were cultured in an incubator with 5% CO<sub>2</sub>, 5% O<sub>2</sub>, and 37°C with daily medium exchanges.

### 2.2 | Axial compression bioreactor

As the IVD is dynamically loaded in vivo, we developed a novel force-controlled axial compression bioreactor to dynamically load NP explants (Figure 1B). The bioreactor system fits into a conventional incubator. The bioreactor is motorized by an electric actuator (LEY32C, SMC, Eindhoven, Netherlands) with I/O controller (LECP6, SMC). Via serial connection, the controller is connected to a computer with a custom written MatLab (R2018b, MathWorks, Natick, MA, USA) graphical user interface, movement is controlled by Modbus communication. By dynamically moving the actuator in displacement control, stainless steel tension springs (Amatec, Alphen aan den Rijn, the Netherlands) with a known spring constant are extended and relaxed (Figure 1C). The resulting pressure is known due to the defined surface area of the NP explants. The pressure signal is measured with load cells (Tinytronics, Eindhoven, the Netherlands), amplified and digitalized (HX711, Tinytronics) and acquired with a microcontroller (Arduino Nano Every, Arduino, Somerville, MA,

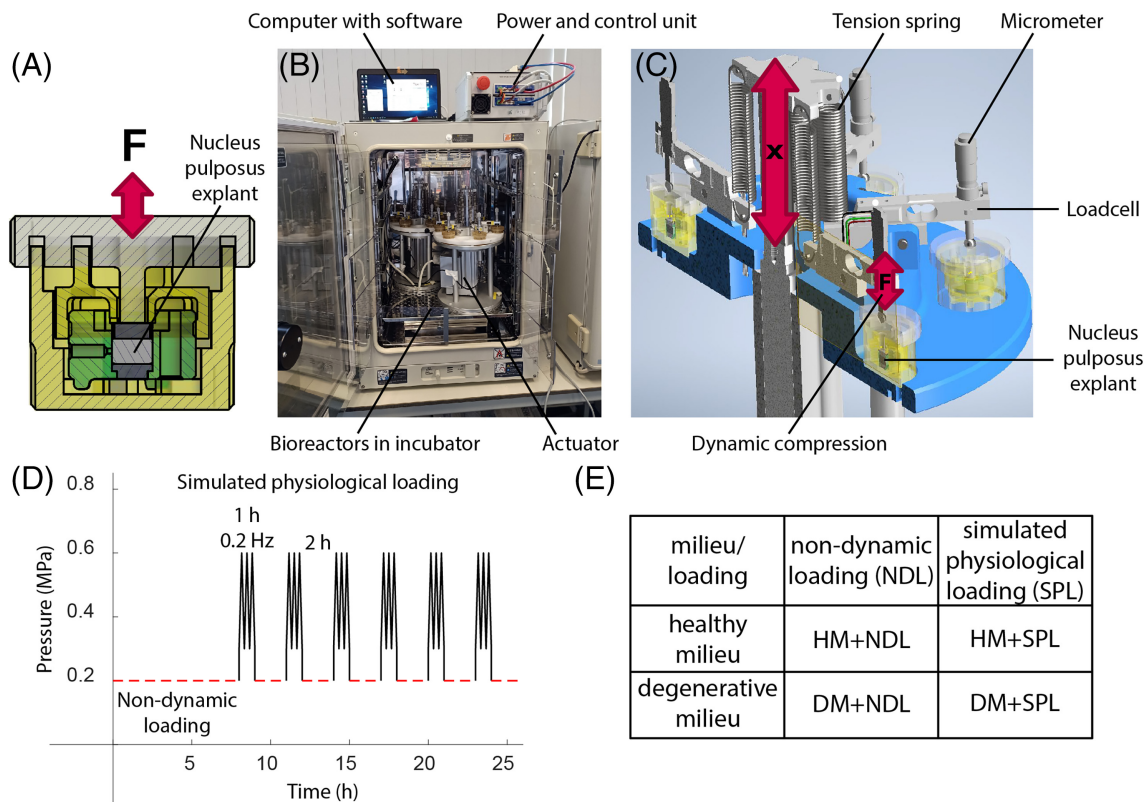


**FIGURE 1** Bovine nucleus pulposus (NP) explants in healthy and degenerative milieu. (A) Two axial compression bioreactor units with spots for six explants each fit into a conventional incubator. A custom-written Matlab software is connected to the controller that regulates the dynamic movement of the electric actuators. (B) During the dynamic movement, tension springs with a known spring rate are extended to a preset pressure. The force can be measured with a loadcell and finetuned with a micrometer (to adjust for sample height). (C) The NP explants are dynamically axially compressed in a previously developed volume controllable NP culture chamber. (D) The explants were either cultured with nondynamic loading (NDL) or with simulated physiological loading (SPL) in a healthy (HM) or degenerative milieu (DM), (E) resulting in four groups: HM + NDL, HM + SPL, DM + NDL and DM + SPL. F, force; x, displacement

**TABLE 1** Culture medium mimicking a healthy or degenerative milieu

Healthy milieu	Degenerative milieu
5% CO <sub>2</sub> /O <sub>2</sub> , 37°C, 3% fetal bovine serum	
3 mM glucose	1 mM glucose
pH 7.1	pH 6.8

USA). Twelve explants can be loaded simultaneously with up to 1 MPa load and a maximum frequency of 1 Hz with pressure ranges of up to  $\pm 0.6$  MPa per cycle.

### 2.3 | Loading

NP explants were equilibrated to 0.2 MPa by applying a static weight overnight. Subsequently, the volume was locked (Day 1) for the entire culture period. This confines explants to a maximal swelling of this volume while still enabling additional dynamic compression. Afterwards, explants were loaded for 6 days (to Day 7). During nondynamic

loading, volume-confined samples were not additionally loaded, that is, they remained at a volume that reflects the adjusted 0.2 MPa (Figure 1D). Simulated physiological loading consisted of 6 h nondynamic loading followed by 18 h of intermittent dynamic loading (6 cycles of: 1 h of 0.3–0.6 MPa at 0.2 Hz (square wave), and 2 h nondynamic loading). These simulated physiological loading parameters led to NP compression of 10%–20% (data not shown), which is the expected height loss of a diurnal cycle due to the fluid loss and reimpement.<sup>30,31</sup> The combination of environment (healthy and degenerative milieu, HM and DM) and loading (simulated physiological and nondynamic loading, SPL and NDL) resulted in explants being cultured at one of these four conditions: HM + NDL, HM + SPL, DM + NDL, and DM + SPL (Figure 1E); the groups were compared to NP tissue harvested on Day 0, which we will refer to as “native”.

### 2.4 | Sample harvest

Explants were harvested on Day 0 before culture ( $n = 6$ , “native”) or on Day 7 ( $n = 6$ /group). Explants were cryopreserved by plunging into liquid nitrogen to maintain the shape. The frozen samples were cut



with a razor blade at room temperature to obtain  $\frac{1}{2}$  for histology,  $\frac{1}{4}$  for biochemical analysis and the remaining  $\frac{1}{4}$  was cut into upper, core, and lower region for glucose and lactate determination in the tissue. Additionally, on Day 2 ( $n = 3$ ) explants were harvested and  $\frac{1}{2}$  was obtained for histology and  $\frac{1}{2}$  for lactate and glucose measurements in the tissue. For histological analysis, samples were covered in Tissue-Tek (Sakura, Alphen aan den Rijn, the Netherlands), frozen on dry ice, and stored at  $-20^{\circ}\text{C}$ . Medium supernatant samples were taken daily before medium changes and stored at  $-20^{\circ}\text{C}$  until further analysis. Samples for biochemical as well as lactate and glucose analysis were weighed to obtain wet weight and subsequently stored at  $-80^{\circ}\text{C}$  and once frozen lyophilized for 72 h, after which dry weight was determined. Dehydrated samples were digested for 16 h at  $60^{\circ}\text{C}$  in digestion buffer (100 mM phosphate buffer, 5 mM L-cystein, 5 mM EDTA) containing 140  $\mu\text{g}/\text{ml}$  papain (P-5306).<sup>32</sup>

## 2.5 | Histological analysis

Cryosections with 8  $\mu\text{m}$  thickness were collected (CM1950, Leica Biosystems, Nußloch, Germany) on Superfrost™ plus Adhesion Microscope slides (Gerhard Menzel GmbH, Braunschweig, Germany) and stored at  $-20^{\circ}\text{C}$ . Before staining, sections were incubated at  $37^{\circ}\text{C}$  for 30 min to increase adherence. Lactate dehydrogenase (LDH) staining was performed to visualize viable cells.<sup>33</sup> Shortly, 10 ml of a reaction mix were prepared containing 40% Polypep (P5115), 66 mg Glycine-Glycine (G3915), 180  $\mu\text{l}$  (+) lactic acid (69771), 17.5 mg  $\beta$ -nicotinamide adenine dinucleotide (43410) and, after adjusting to pH 8, 30 mg nitroblue tetrazolium (N5514) was added. Sections were covered with reaction mix and incubated for 4 h protected from light at  $37^{\circ}\text{C}$ . Reaction mix was removed by washing sections in lukewarm water, after which samples were fixed in 70% ethanol for 5 min. To stain proteoglycans, sections were fixed in 3.7% formalin for 5 min, hydrated in water for 5 min and stained with Alcian Blue for 30 min. Sections were imaged with a bright-field microscope (Axio Observer Z1, Zeiss, Germany). To determine the viable cell density (VCD, [cells/ $\text{mm}^2$ ]), cells positively stained with LDH (blue cytoplasmic staining) were counted in a blinded fashion in the upper and lower (i.e., peripheral), and core regions of each explant. Three 1  $\text{mm}^2$  areas per each region (i.e., 9 areas per sample) were counted and averaged, resulting in 3 averaged measurements per sample (top, core, and bottom). The VCD measurements in cells/ $\text{mm}^2$  were not converted to volume in, e.g. cells/ml, to prevent conversion errors.

## 2.6 | Biochemical analysis

Water content of the explants was calculated from the wet weight and dry weight. Hydroxyproline (HYP) content was measured with a chloramine-T assay<sup>34</sup> using trans-4-hydroxyproline (H5534) as standard. Absorbance was read at 550 nm. sGAG content was determined by 1,9-dimethylmethylene blue (DMMB) binding assay at pH 3 using

chondroitin sulfate from shark cartilage (C4348) as standard.<sup>35</sup> The absorbance at 595 nm was extracted from 540 nm. HYP and sGAG were normalized by dry weight. The fixed charge density (FCD), in mEq/g wet tissue, was calculated from the measured sGAG content (g), assuming a molecular weight of 502.5 g/mol for CS and a quantity of charge of 2 moles of charge per mole of sGAG.<sup>36,37</sup>

## 2.7 | Lactate and glucose assay

Spatial distribution of glucose and lactate concentration was measured in the upper, core, and lower region of the tissue explants that were digested in papain digestion buffer as described above. Additionally, glucose and lactate concentrations were measured in the medium supernatants to determine the metabolic activity of cells. Glucose concentrations were measured with an adapted colorimetric assay.<sup>38,39</sup> Shortly, a fresh buffer/chromophore reagent was prepared by mixing 3.5 ml of 10 mM 4-aminoantipyrine (06800) with 3.5 ml of 10 mM 3-(N-ethyl-3-methylanilino) propane sulfonic acid sodium salt (E8506) and 3 ml of 0.8 M sodium phosphate buffer (pH 6). To prepare the assay reagent, 100  $\mu\text{l}$  buffer/chromophore reagent were mixed with 10  $\mu\text{l}$  peroxidase from horseradish (1.6 U/ml, 77 332) and 10  $\mu\text{l}$  of glucose oxidase (2.7 U/ml, G7141) per sample. In each well of a transparent 96-well plate, 2  $\mu\text{l}$  of sample or standard were added to which 120  $\mu\text{l}$  of the freshly prepared assay reagent were added to initiate the reaction. Samples were incubated for 30 min at room temperature in the dark and absorbance was measured at 550 nm. Glucose concentrations were calculated via a standard curve of D-glucose (15023-021, Fisher Scientific, Waltham, MA, USA) ranging from 0.08 to 5 mM. Lactate concentrations were measured based on an enzymatic assay.<sup>40</sup> Shortly, a reaction mix was prepared containing 5 mg/ml of  $\beta$ -nicotinamide adenine dinucleotide hydrate (N7004), 0.2 M glycine buffer (G5418), and 22.25 U/ml of L-lactic dehydrogenase from bovine heart (L3916). Subsequently, 40  $\mu\text{l}$  of sample were mixed with 40  $\mu\text{l}$  reaction mix in a well of a transparent 96-well plate. The plate was incubated at  $37^{\circ}\text{C}$  for 30 min and absorbance was measured at 340 nm. The lactate concentration of the samples was calculated using a standard curve of sodium L-lactate (L7022) ranging from 0.016 to 1 mM.

## 2.8 | Statistical analysis

Statistical analysis was performed with GraphPad Prism 9.1.0. Normal distribution of residuals was tested with a Shapiro–Wilks' test. Results are presented as mean  $\pm$  one standard deviation. For normally distributed data, (repeated measure) one-way or two-way analysis of variance with Tukey's multiple comparison post hoc test was used to test for significance between factor levels. When data were nonparametric, Kruskal–Wallis test with Dunn's multiple post hoc comparison test was performed. Statistical significance was assumed for  $p < .05$ .

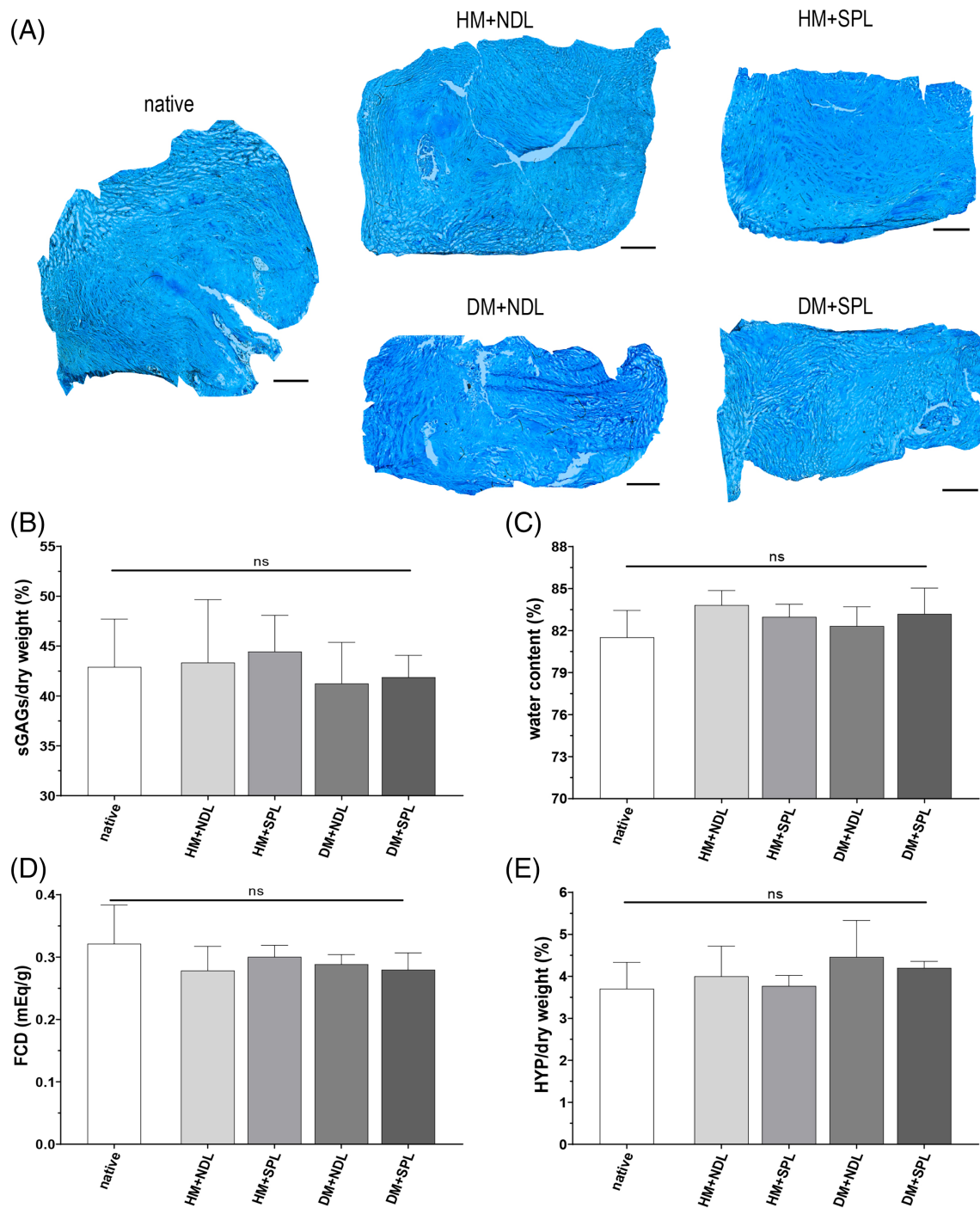


**FIGURE 2** Extracellular matrix composition after 7 days in culture analyzed by proteoglycan staining and biochemical analysis. (A) The Alcian Blue staining intensity was comparable in all groups. (B) The sulphated glycosaminoglycan (sGAG) content, (C) water content, and (D) the resulting fixed charge density (FCD) were not significantly changed. (E) The hydroxyproline (HYP) content did not significantly change. DM, degenerative milieu; HM, healthy milieu; NDL, nondynamic loading; ns, nonsignificant; SPL, simulated physiological loading. Scale bars: 1 mm

### 3 | RESULTS

#### 3.1 | Loading and chemical milieu did not affect the extracellular matrix composition

After culturing the explants for 7 days, there were no gross-morphological differences observed. The Alcian Blue staining intensity,

an indication of proteoglycan content, was in all treatment groups comparable to native tissue, that is, freshly harvested NP tissue (Figure 2A). The sulphated glycosaminoglycan (sGAG) content (Figure 2B), the major extracellular matrix (ECM) component of the NP, did not change and neither did the water content (Figure 2C) or the resulting FCD (Figure 2D). The HYP content, an indication of the collagen content, remained comparable to native tissue (Figure 2E). All in all, there were no significant

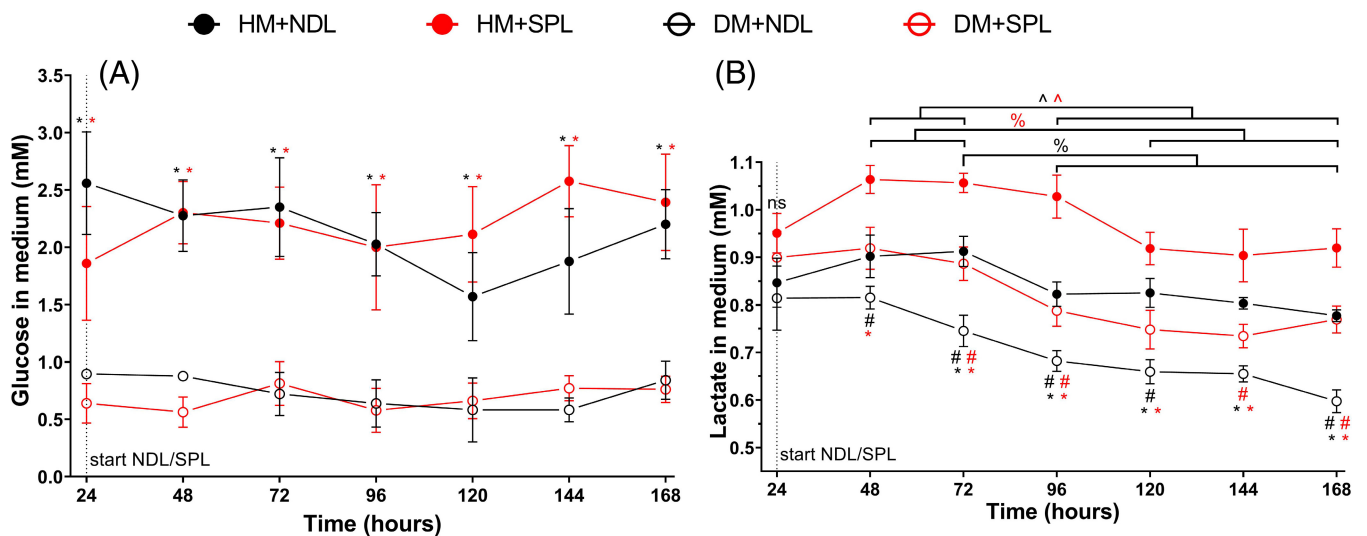


**FIGURE 3** Glucose and lactate concentrations in medium measured by colorimetric and enzymatic assays. (A) The glucose concentration was higher in healthy milieu (HM) groups with medium containing 3 mM glucose compared to degenerative milieu (DM) groups with medium containing 1 mM glucose. (B) The lactate concentration in the medium was higher in groups with simulated physiological loading (SPL) compared to the nondynamic loading (NDL) groups with the same milieu. Lactate concentration was decreased at later timepoints compared to earlier timepoints. In HM groups, lactate concentration was increased at most time points compared to DM groups.  $n = 6$ /group. Statistically significant differences: \*between HM and DM in NDL (black) and SPL (red); #between NDL and SPL in HM (black) and DM (red); ^over time in DM with NDL (black) and SPL (red); % over time in HM with NDL (black) and SPL (red); ns, nonsignificant

differences observed in the ECM content between any of the studied groups. Furthermore, all explants regained their height corresponding to the equilibrated 0.2 MPa within the 8 h of nondynamic loading in the diurnal cycle (data not shown).

### 3.2 | Dynamic loading increased lactate production

Lactate and glucose concentrations were determined in the medium samples harvested each day. Due to the higher medium glucose concentration in healthy milieu compared to degenerative milieu groups (3 mM vs. 1 mM, respectively), healthy milieu medium supernatants contained correspondingly significant more glucose than that of degenerative milieu at all time points (Figure 3A). There was no significant difference in medium glucose concentration between the simulated physiological and nondynamic loading groups for the same medium type, however, medium glucose concentration reached critical levels for cell survival, that is, 0.5 mM,<sup>13,14</sup> in the degenerative milieu groups. The lactate released into the medium was significantly higher in groups loaded with simulated physiological compared to nondynamic loading groups ( $p \leq 0.05$ , Figure 3B) in both milieus. At later timepoints, lactate release was significantly decreased compared to earlier timepoints ( $p \leq 0.05$ ). Lactate concentrations in medium of healthy milieu groups were significantly increased compared to degenerative milieu groups ( $p \leq 0.05$ ).

### 3.3 | Viable cell density was reduced in the core NP in dynamic loading conditions

The viable cell density (VCD, cells/mm<sup>2</sup>) was measured with a lactate dehydrogenase (LDH) staining. Metabolically active cells had a blue-

purple formazan salt visible in the cytoplasm. The VCD in the periphery, i.e. in the upper and lower regions, was not different on Day 2 (Figure 4A) or Day 7 (Figure 4B) between any group and was not reduced with respect to the native NP tissue. While the VCD in the core region was not changed on Day 2 (Figure 4C), there was a significant reduction of VCD in both simulated physiological loading groups on Day 7 of approximately 40%–50% ( $p \leq 0.01$ , Figure 4D) compared to the native NP. The VCD in the degenerative milieu with simulated physiological loading (DM + SPL) group was additionally significantly reduced compared to the healthy milieu with nondynamic loading (HM + NDL) group by circa 40%. There was no gradient formation of VCD on Day 2 (Figure 4E). On Day 7, the reduced VCD in the core compared to the constant VCD in the periphery led to a gradient formation in the degenerative milieu with simulated physiological loading (DM + SPL) that was significantly lower (around 35%) than the native and healthy milieu with nondynamic loading (HM + NDL) group ( $p \leq 0.05$ , Figure 4F) and which is visible in a heatmap-like plot (Figure 4G).

### 3.4 | Lactate tissue levels are reduced in explants cultured in degenerative milieu

Glucose and lactate were measured in tissue samples harvested on Day 2 and on Day 7 in the upper, core, and lower region of the NP explant. There was no gradient measured in either lactate (Figure 5A) or glucose (Figure 5B) in the NP tissue at Day 2 or 7 in any group. The lactate concentration in native tissue (Figure 5C) was around 6 mM. In both degenerative milieu groups, lactate was significantly reduced compared to the native tissue, on Day 2 and Day 7 to around 2 mM.

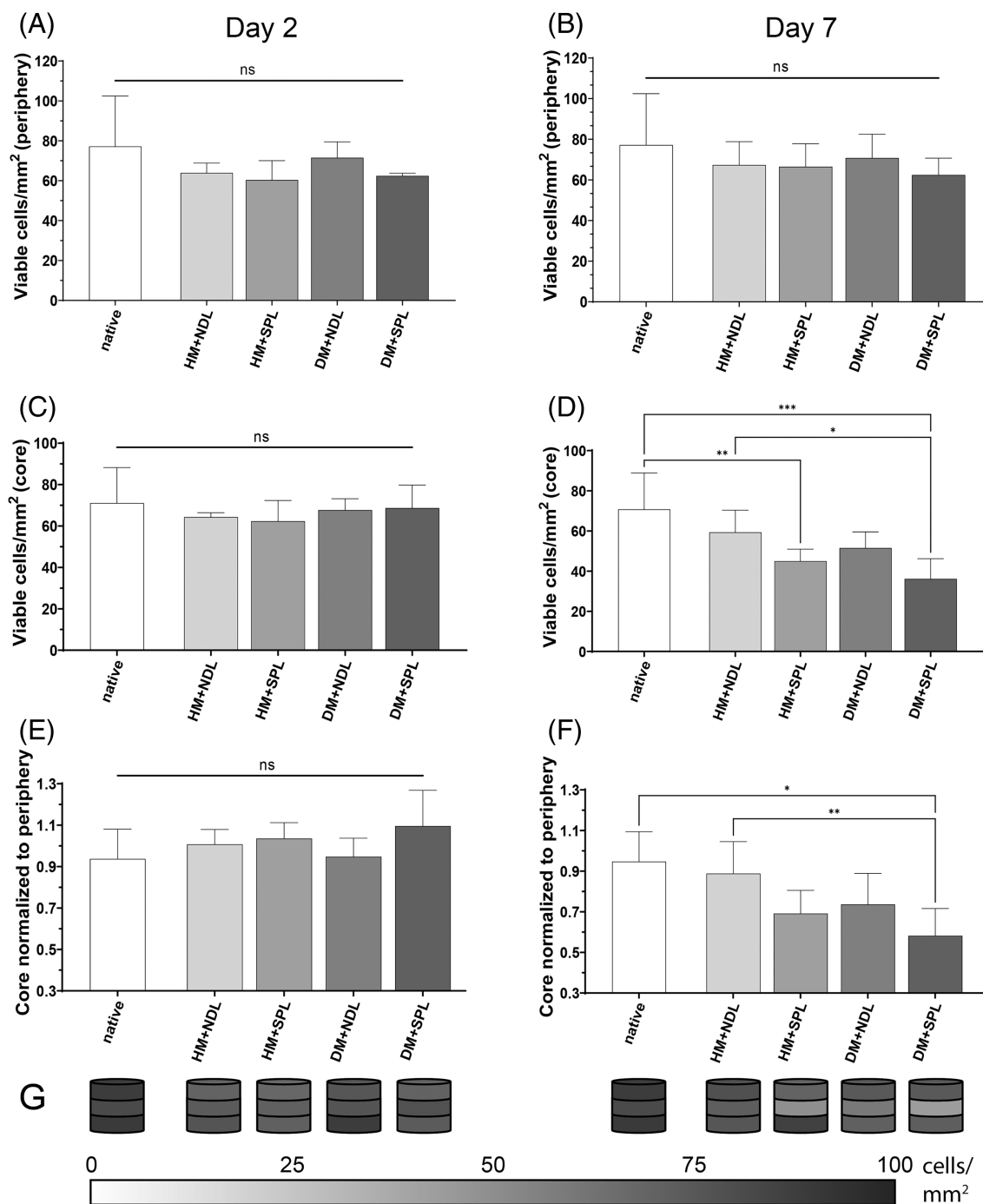


**FIGURE 4** Spatial distribution of viable cells in bovine nucleus pulposus explants measured by lactate dehydrogenase staining. The viable cells in the periphery were not changed on both, (A) Day 2 and (B) Day 7. The viable cells in the NP core were unchanged on (C) Day 2 but reduced in both, HM + SPL and DM + SPL groups, on (D) Day 7 compared to the native group. (E) There was no gradient formation on Day 2. (F) On Day 7, there was a gradient formation in the DM + SPL group. (G) Heatmap plots of the 3 regions of the NP show the reduced viable cells/mm<sup>2</sup> graphically. DM, degenerative milieu; HM, healthy milieu; NDL, nondynamic loading; SPL, simulated physiological loading. \* $p < 0.05$ ; \*\* $p < 0.01$ ; \*\*\* $p < 0.001$ ; ns, nonsignificant;  $n = 3$ /group (Day 2),  $n = 6$ /group (native and Day 7)

However, in the healthy milieu groups, lactate was around 4 mM and only significantly reduced in the healthy milieu with nondynamic loading (HM + NDL) group on Day 7 compared to the native tissue. Additionally, lactate was significantly reduced in the degenerative milieu groups compared to the healthy milieu groups on Day 7. The glucose

concentration in the tissue (Figure 5D) was in the range of around 0.2–0.6 mM in all groups and in the native tissue. On Day 7, glucose in the healthy milieu with simulated physiological loading (HM + SPL) group was significantly increased compared to the native, Day 2 healthy milieu with simulated physiological loading (HM + SPL) as

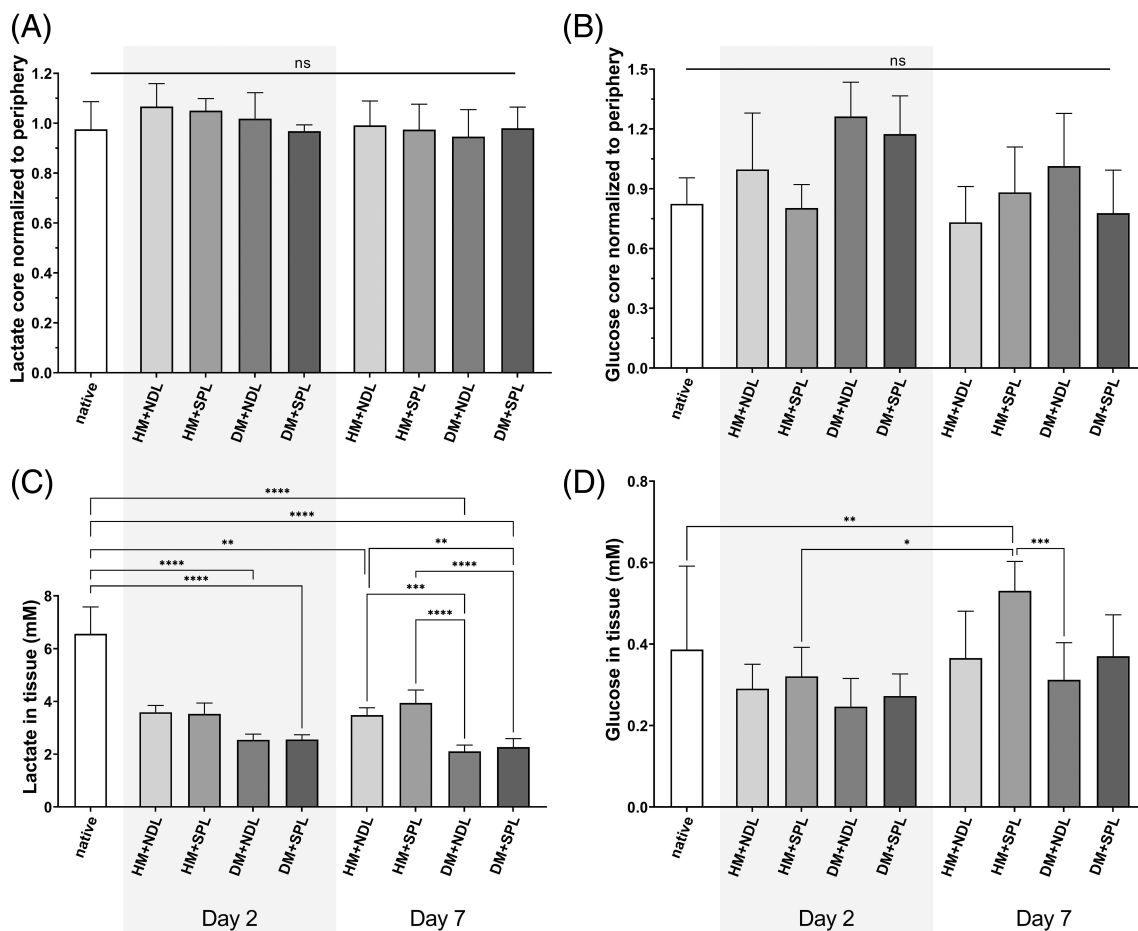


**FIGURE 5** Lactate and glucose concentrations in tissue measured by colorimetric and enzymatic assays. There was no gradient formation of (A) lactate and (B) glucose inside the tissue. (C) Lactate concentration was reduced after 2 and 7 days in the degenerative milieu (DM) groups compared to the native concentration. On Day 7, lactate was reduced in DM compared to HM milieus. (D) The glucose concentration reached critical values for cell survival in all groups. On Day 7, there was a significant increase in the HM + SPL and DM + NDL group compared to the native tissue and the Day 7 HM + SPL and DM + NDL group. DM, degenerative milieu; HM, healthy milieu; NDL, nondynamic loading; SPL, simulated physiological loading. \* $p < 0.05$ ; \*\* $p < 0.01$ ; \*\*\* $p < 0.001$ ; \*\*\*\* $p < 0.0001$ ; ns, nonsignificant.  $n = 3$ /group (Day 2),  $n = 6$ /group (native and Day 7)

well as degenerative milieu with nondynamic loading (DM + NDL) Day 7 groups. Glucose tissue concentrations were not significantly different in any of the remaining groups and time points.

## 4 | DISCUSSION

NP cells, in their *in situ* tissue environment, could survive under harsh conditions such as low glucose, oxygen, and pH when cultured *in vitro*. Here, we demonstrated, that dynamic loading led to increased cellular metabolic activity in *ex vivo* cultured NP explants as evidenced by their increased production of lactate. Furthermore, when explants were cultured in a nutrient milieu that mimics the conditions found in the inner annulus fibrosus of human degenerative discs, dynamic loading was an additional stressor that reduced the cell density in the core of NP explants, so much so that a gradient formed from the periphery to the core after 7 days. There was no gradient formation in tissue levels of glucose and lactate, indicating their quick equilibration.

### 4.1 | A dynamically loaded NP explant culture

The biggest obstacle for successful NP tissue cultures is its high osmotic potential. This leads to considerable swelling when unconstrained in culture and therefore needs to be counteracted. Recently, we developed a bioreactor chamber that controls swelling and enables compressive loading.<sup>6,23</sup> However, dynamic loading is essential for cellular homeostasis of disc cultures.<sup>41,42</sup> Therefore, we developed a bioreactor which allows us to additionally apply axial dynamic compressive loading to the NP explants.

Loading parameters that dictate cell and tissue homeostasis are model dependent and therefore need to be adjusted to the specific research question. Overload and immobilization in terms of magnitude, frequency, and duration of loading can be detrimental for the disc<sup>41,42</sup> and several studies have shown reduced cell viability after overloading.<sup>42-44</sup> To prevent overloading-induced cell death, the loading parameters in this study were chosen based on suggested physiological magnitudes and frequencies for IVD cultures,<sup>42,45</sup> previous studies,<sup>43,44</sup> and the range of pressures measured during normal



activity in the human and bovine lumbar disc.<sup>46,47</sup> Haglund et al. reported a reduced cell viability in bovine discs after 10 days of culture at loading parameters comparable to ours but with a higher pressure range (0.1–0.6 MPa).<sup>48</sup> In our study, we did not observe differences in the VCD in the periphery of the NP tissue (healthy milieu with simulated physiological loading compared to native). This difference between studies could be a result of differences in the culture platform, that is, IVD organ culture versus NP tissue culture, or loading range. In our study, we did though observe a gradient in VCD going from the periphery to the center of the tissue (healthy milieu with simulated physiological loading). This spatial response is not expected to result from the magnitude of loading alone, as compressive loading leads to an equal distribution of compressive stress in all directions and through the NP tissue.<sup>49</sup> In addition, similar and even larger VCD gradients under degenerative milieu conditions with simulated physiological loading support our conclusions on the role of dynamic loading leading to increased metabolic needs not compatible with the nutrient supply conditions. Nevertheless, the intradiscal pressures at rest and activity of bovine coccygeal discs were, to the best of our knowledge, not reported yet. We expect those pressures to be lower than in the lumbar spine, as the tail does not carry the upper body weight like human lumbar spines and is not involved in the stabilization of the quadruped's spine.

## 4.2 | The ECM composition is not affected by the culture conditions

In this study, there were no differences detectable in the ECM composition of the explants for the different culture conditions, neither qualitatively by an Alcian Blue staining, nor quantitatively by biochemically evaluating the main components of the NP's ECM. The glucose measured in tissue was within the range of glucose concentrations reported from computational studies in degenerative human conditions (median 1 mM<sup>50</sup>). The lactate measured here in native bovine tissue (around 6 mM) is in agreement with the lactate concentration reported in human NP tissue (5–10 mM<sup>51</sup>), which corresponds approximately to pH 7,<sup>17</sup> the median value of degenerated discs.<sup>50</sup> Additionally, all dynamically loaded samples were able to regain the height corresponding to the equilibrated 0.2 MPa within the 8 h of unloading. Overall, this indicates that the ECM, and thereby biomechanical function,<sup>6,36</sup> remained unchanged for at least 1 week in culture in all studied conditions. This furthermore illustrates that the loading parameters and culture milieu chosen did not induce detectable degenerative changes after 7 days of culture at the tissue level.

## 4.3 | Cell density reduction and nutrient/metabolite conditions in the NP

To the best of our knowledge, this is the first study to show a reorganization of VCD in the NP core after physiological-like dynamic

loading. The reduction of VCD in the NP core compared to the periphery in dynamically loaded groups additionally led to a gradient formation of VCD in the degenerative milieu. Additionally, when explants were cultured with dynamic loading, the lactate produced by glycolysis and released into the medium was increased compared to their unloaded counterparts, regardless of nutrient milieu, indicating an increased cellular metabolic activity. An increase in lactate production has also been observed in whole porcine notochordal cell-rich IVDs, when they were dynamically loaded for 1 h compared to static loaded controls.<sup>52</sup>

As there were no changes in VCD detected on Day 2, cell death must have occurred between Day 4 and Day 7. The LDH enzyme can remain stable for up to 36 h after cell death which means that the VCD on Day 2 of this study mainly reflects the initial explant culture, and Day 7 reflects VCD after several days in culture. This could potentially correlate to a decrease of lactate concentration measured in medium over time, which indicates that metabolic activity might have been reduced at about 3–4 days of culture. Comparatively, when NP cells were cultured in glucose-free medium in alginate beads, viable cells were still found even after 24 h, supporting the hypothesis that it takes several days of harsh conditions to reduce cell viability.<sup>53</sup> Similarly, when IVD organs were cultured in a nutrient-deprived environment (2 g/L glucose, i.e., 11.1 mM), cell viability was reduced by around 50% within days, after which the cell concentration remained stable for 3 weeks.<sup>12</sup>

Although it was clear that higher VCD gradients had formed when cells were mechanically stimulated and under more restrictive nutrient environments, we did sometimes also observe small differences in VCD between the top and bottom peripheries (Figure 4G). This could have been due to slight differences in nutrient supply conditions between top and bottom periphery of the tissue induced by the asymmetric geometry of the bioreactor chambers. However, as these differences were within the standard deviations of the VCD of the periphery regions within in each experimental group, this was not considered significant.

The culture milieus in this study aimed to replicate the human NP environment in healthy and diseased IVDs, that is, that of the inner annulus fibrosus. Low glucose and low pH are considered to be the key parameters that control cell density in the IVD. Therefore, they were chosen as control parameters in this study. A nutrient gradient, due to diffusive transport from the vasculature to the central NP as well as consumption by the cells, is believed to cause a reduction in cell viability.<sup>2,8</sup> In line with this, in an artificial cartilage endplate/NP culture system, a cell viability gradient was observed, where a higher cell density had a higher glucose demand, which led to a lower cell density with increasing distance from the glucose supply.<sup>54</sup> While the glucose concentration remained roughly at 2.5 mM in the healthy milieu, it was near the critical value of 0.5 mM in the degenerative milieu reported to lead to NP cell death.<sup>13,14</sup> This means that in degenerative milieu conditions, glucose levels reached critical values even in the peripheral regions, although, as the VCD was not found to be reduced in these regions, there was enough glucose supply to

support cell survival. However, there were no glucose or lactate gradients in the tissue observed at the 2 timepoints (Day 2 and Day 7). Therefore, we expect that the differences may have been too small to detect with the harvesting and assay methods employed or that gradients were only transient, quickly resolving. While the glucose/lactate gradients can be transient, a reduction in cell density is unlikely to recover without mitogenic therapy even when nutrients are plentiful again, which can lead to reduced cell density while a nutritional gradient would be no longer measured. Nevertheless, gradients are necessary for diffusional transport, and maybe in the NP, very small, transient, gradients drive diffusional transport, even more so in critical nutrient conditions. Additionally, nutrient and metabolite gradients during IVDD might not be linear but could follow regional variations in ECM composition and cell cluster formation.<sup>55,56</sup> Summarizing, we hypothesize that low glucose and low pH together were the cause of cell death in NP cores in this study.

#### 4.4 | NP cell metabolism and cell fate

20% O<sub>2</sub>, which is still used in ca. 90% of *ex vivo* IVD organ cultures,<sup>57</sup> can lead to enhanced reactive oxygen species formation.<sup>58</sup> Additionally, glucose is metabolized to lactate by NP cells even under 20% O<sub>2</sub> conditions,<sup>3,14</sup> and so cellular energy metabolism does not profit from such conditions. While glycolysis is less efficient, it is much faster in ATP production than oxidative phosphorylation, and the glycolysis rate of NP cells was previously estimated to be nearly 100%.<sup>13</sup> Additionally, NP cells express monocarboxylate transporter 4 and LDH-M, enzymes that catalyze lactate export and pyruvate to lactate conversion, respectively.<sup>51</sup> The lactic acid catabolized from glucose readily dissociates to lactate and H<sup>+</sup>. Lactate can thereby either be reconverted to pyruvate via LDH or transported into the extracellular matrix.<sup>59</sup> If the latter occurs, the secreted lactate decreases the pH in the cells' microenvironment.<sup>15-17</sup> Interestingly, in a glucose deprived environment, lactic acidosis, that is, a low pH from a high [lactate], led to cell cycle arrest and autophagy in cancer core cells.<sup>60,61</sup> Similarly, this could also occur with NP cells. Once the cells are deprived of nutrients, they could react very differently and might become senescent, autophagic, apoptotic, necrotic, and so on. Nevertheless, the mechanisms of various cell fates caused by nutrient deprivation and other factors needs further investigation.

#### 4.5 | Relevance for clinical translation and regenerative therapies

There is a controversy of whether regenerative strategies utilizing cell injections or growth factors that induce proliferation are beneficial if nutrition is limited in the harsh microenvironment in the core of the disc.<sup>62</sup> A theoretical evaluation of a regenerative cell concentration injection was recently done by McDonnell and Buckley, who suggest that a high number of injected cells might survive in the disc.<sup>50</sup> However, that would require that those cells are as insensitive to harsh conditions as NP cells, whereas most cell used for intradiscal injection

are more sensitive than mature NP cells to the critical microenvironment in the disc.<sup>63</sup> Alginate constructs containing bone marrow stem cells or NP cells cultured at low glucose (1 mM) and hypoxic conditions (5% O<sub>2</sub>), showed that NP cells are less sensitive to harsher environments, whereas stem cells have shown inhibited sGAG and collagen production and increased cell death. Additionally, a gradient formation in cell viability with lower viability in the core was observed in the stem cell group after 21 days.<sup>64</sup> A promising approach to overcome the sensitivity issue is cellular priming, where cells are cultured in conditions that mimic the NP milieu.<sup>65</sup> Additionally, many biomaterials are currently being investigated for their potential use to protect the injected cells and regenerate the IVD.<sup>66</sup> Nevertheless, we demonstrate that dynamic loading can also affect cell metabolism and that physiological-like loading as well as appropriate nutrient milieu must be applied in IVD organ and explant cultures when cellular therapies are explored. Finally, the IVD size of the studied model in comparison to the human IVD needs to be taken into consideration for a better clinical translation of regenerative therapies.

#### 4.6 | Study limitations

Spatial resolution of cell density, lactate, and glucose concentration assessment was limited by the number of regions chosen, that is, the peripheral and core regions. Furthermore, the specific mechanism of cell death as a response to nutrient starvation and metabolite excess in a dynamic environment was not investigated. In this study we did not measure the pH in the medium due to the buffer system used (sodium bicarbonate/CO<sub>2</sub>), which immediately changes once the medium is exposed to the environment outside the incubator. Nevertheless, the adjusted pHs might have even further decreased during culture due to the increased lactic acid production.<sup>17</sup>

The bovine caudal discs are another study limitation, as translation to the human situation is not straightforward. NP explants were from bovine caudal discs, which are smaller than human lumbar IVDs, and smaller discs allow a higher cell density. In the human NP, the cell density is approximately 2000–4000 cells/ml,<sup>10,11</sup> whereas 2–3 year old bovine NPs used in this study have roughly or 9300 ± 2700 cells/ml (75 ± 22 cells/mm<sup>2</sup>, 8 μm slice thickness, fresh tissue), comparable to previous reports of bovine NP cellularity.<sup>2,57,67,68</sup> The smaller size of the bovine NP could have been responsible for a lack of a cell density gradient in the native bovine NP tissue and also for the small nonsignificant reduction in cell density in the core of the NP with nondynamic loading and healthy nutrient conditions. Nevertheless, the here presented mechanism is expected to be similar in human discs, assuming a similar health state of the cells at the baseline.

Furthermore, IVDD in humans is more complex than the here presented model. For example, a pro-inflammatory environment can additionally be involved in cell metabolism and cellular fate.<sup>69</sup> Therefore, future studies that mimic the degenerative disc

environment should also consider investigation of the inflammatory milieu.

## 4.7 | Conclusion

In this study, we demonstrated that NP cells in an explant culture can survive even under very harsh conditions with critical nutrient supply, low oxygen tension, and low pH. Dynamic loading increases the metabolic activity of NP cells. When combined with a harsh nutrient environment found in degenerated discs, a new distribution with less viable cells within the NP tissue core is created. This should be considered for cell injections and therapies that lead to cell proliferation for treatment of IVD disease.

## AUTHOR CONTRIBUTIONS

All authors contributed to research design and contributed to the bioreactor design and development. ES acquired data. All authors analyzed and interpreted data. ES and KI drafted the manuscript and all authors revised it critically. All authors have read and approved the final submitted manuscript.

## ACKNOWLEDGMENTS

This project received funding from the European Union's Horizon 2020 research and innovation program iSpine under the grant agreement #825925 ([www.ipspine.eu](http://www.ipspine.eu)). MAT receives financial support from the Dutch Arthritis Society (LLP22).

## CONFLICT OF INTEREST

The authors declare no conflicts of interest.

## ORCID

Elias Salzer  <https://orcid.org/0000-0001-8711-4243>

Marianna A. Tryfonidou  <https://orcid.org/0000-0002-2333-7162>

Keita Ito  <https://orcid.org/0000-0002-7372-4072>

## REFERENCES

- Ravindra VM, Senglaub SS, Rattani A, et al. Degenerative lumbar spine disease: estimating global incidence and worldwide volume. *Glob Spine J*. 2018;8(8):784-794.
- Urban JPG, Smith S, Fairbank JCT. Nutrition of the intervertebral disc. *Spine (Phila Pa 1976)*. 2004;29(23):2700-2709.
- Holm S, Maroudas A, Urban JPG, Selstam G, Nachemson A. Nutrition of the intervertebral disc: solute transport and metabolism. *Connect Tissue Res*. 1981;8(2):101-119.
- Zhu Q, Gao X, Levene HB, Brown MD, Gu W. Influences of nutrition supply and pathways on the degenerative patterns in human intervertebral disc. *Spine (Phila Pa 1976)*. 2016;41(7):568-576.
- Walter BA, Likhitanichkul M, Illien-Junger S, Roughley PJ, Hecht AC, Iatridis JC. TNF $\alpha$  transport induced by dynamic loading alters biomechanics of intact intervertebral discs. *PLoS One*. 2015; 10(3):e0118358.
- Salzer E, Mouser VHM, Tryfonidou MA, Ito K. A bovine nucleus pulposus explant culture model. *J Orthop Res*. 2021;40(9):2089-2102.
- Urban JPG. The role of the physicochemical environment in determining disc cell behaviour. *Biochem Soc Trans*. 2002;30(6):858-864.
- Huang YC, Urban JPG, Luk KDK. Intervertebral disc regeneration: do nutrients lead the way? *Nat Rev Rheumatol*. 2014;10(9):561-566.
- Nachemson A, Lewin T, Maroudas A, Freeman MAR. In vitro diffusion of DYE through the end-plates and the annulus fibrosus of human lumbar intervertebral discs. *Acta Orthop Scand*. 1970;41: 589-607.
- Liebscher T, Haefeli M, Wuertz K, Nerlich AG, Boos N. Age-related variation in cell density of human lumbar intervertebral disc. *Spine (Phila Pa 1976)*. 2011;36(2):153-159.
- Maroudas A, Stockwell R, Nachemson A, Urban J. Factors involved in the nutrition of the human lumbar intervertebral disc: cellularity and diffusion of glucose in vitro. *J Anat*. 1975;120(1):113-130.
- Jünger S, Gantenbein-Ritter B, Lezou P, Alini M, Ferguson SJ, Ito K. Effect of limited nutrition on in situ intervertebral disc cells under simulated-physiological loading. *Spine (Phila Pa 1976)*. 2009;34(12): 1264-1271.
- Bibby SRS, Jones DA, Ripley RM, Urban JPG. Metabolism of the intervertebral disc: effects of low levels of oxygen, glucose, and pH on rates of energy metabolism of bovine nucleus pulposus cells. *Spine (Phila Pa 1976)*. 2005;30(5):487-496.
- Horner HA, Urban JP. 2001 Volvo award winner in basic science studies: effect of nutrient supply on the viability of cells from the nucleus pulposus of the intervertebral disc. *Spine (Phila Pa 1976)*. 2001;26(23):2543-2549.
- Diamant B, Karlsson J, Nachemson A. Correlation between lactate levels and pH in discs of patients with lumbar rhizopathies. *Experientia*. 1968;24:1195-1196.
- Razaq S, Wilkins RJ, Urban JPG. The effect of extracellular pH on matrix turnover by cells of the bovine nucleus pulposus. *Eur Spine J*. 2003;12(4):341-349.
- Mokhbi Soukane D, Shirazi-Adl A, Urban JPG. Computation of coupled diffusion of oxygen, glucose and lactic acid in an intervertebral disc. *J Biomech*. 2007;40(12):2645-2654.
- Grunhagen T, Wilde G, Mokhbi Soukane D, Shirazi-Adl SA, Urban JPG. Nutrient supply and intervertebral disc metabolism. *J Bone Jt Surg*. 2006;88(A):30-36.
- Bibby SRS, Urban JPG. Effect of nutrient deprivation on the viability of intervertebral disc cells. *Eur Spine J*. 2004;13(8):695-701.
- Li H, Liang C, Tao Y, et al. Acidic pH conditions mimicking degenerative intervertebral discs impair the survival and biological behavior of human adipose-derived mesenchymal stem cells. *Exp Biol Med*. 2012; 237(7):845-852.
- Gilbert HTJ, Hodson N, Baird P, Richardson SM, Hoyland JA. Acidic pH promotes intervertebral disc degeneration: acid-sensing ion channel-3 as a potential therapeutic target. *Sci Rep*. 2016;6 (37360):1-12.
- Fernando HN, Czamanski J, Yuan T-Y, Gu W, Salahadin A, Huang CYC. Mechanical loading affects the energy metabolism of intervertebral disc cells. *J Orthop Res*. 2011;29(11):1634-1641.
- Arkesteijn ITM, Mouser VHM, Mwale F, van Dijk B, Ito K. A well-controlled nucleus pulposus tissue culture system with injection port for evaluating regenerative therapies. *Ann Biomed Eng*. 2015;44(5): 1798-1807.
- Mokhbi Soukane D, Shirazi-Adl A, Urban JPG. Investigation of solute concentrations in a 3D model of intervertebral disc. *Eur Spine J*. 2009; 18(2):254-262.
- Nachemson A. Intradiscal measurements of pH in patients with lumbar rhizopathies. *Acta Orthop*. 1969;40(1):23-42.
- Jackson AR, Huang C-YC, Brown MD, Gu WY. 3D finite element analysis of nutrient distributions and cell viability in the intervertebral disc: effects of deformation and degeneration. *J Biomech Eng ASME*. 2011;133(9):091006.
- Magnier C, Boiron O, Wendling-Mansuy S, Chabrand P, Deplano V. Nutrient distribution and metabolism in the intervertebral disc in the unloaded state: a parametric study. *J Biomech*. 2009;42(2):100-108.

28. Ohshima H, Urban JP. The effect of lactate and pH on proteoglycan and protein synthesis rates in the intervertebral disc. *Spine (Phila Pa 1976)*. 1992;17(9):1079-1082.
29. Ishihara H, Urban JPG. Effects of low oxygen concentrations and metabolic inhibitors on proteoglycan and protein synthesis rates in the intervertebral disc. *J Orthop Res*. 1999;17(6):829-835.
30. Wuertz K, Urban JPG, Klasen J, et al. Influence of extracellular osmolarity and mechanical stimulation on gene expression of intervertebral disc cells K. *J Orthop Res*. 2007;25(11):1513-1522.
31. Urban JP, McMullin JF. Swelling pressure of the lumbar intervertebral discs: influence of age, spinal level, composition, and degeneration. *Spine (Phila Pa 1976)*. 1988;13(2):179-187.
32. Kim YJ, Sah RLY, Doong JYH, Grodzinsky AJ. Fluorometric assay of DNA in cartilage explants using Hoechst 33258. *Anal Biochem*. 1988;174(1):168-176.
33. Stoddart MJ, Furlong PI, Simpson A, Davies CM, Richards RG. A comparison of non-radioactive methods for assessing viability in ex vivo cultured cancellous bone: technical note. *Eur Cell Mater*. 2006;12:16-25.
34. Huszar G, Maiocco J, Naftolin F. Monitoring of collagen and collagen fragments in chromatography of protein mixtures. *Anal Biochem*. 1980;105(1):424-429.
35. Farnadale RW, Sayers CA, Barrett AJ. A direct spectrophotometric microassay for sulphated glycosaminoglycans in cartilage cultures. *Connect Tissue Res*. 1982;9:247-248.
36. Urban JPG, Maroudas A. The measurement of fixed charged density in the intervertebral disc. *Biochim Biophys Acta*. 1979;586(1):166-178.
37. Jackson AR, Yuan T-Y, Huang C-Y, Gu WY. A conductivity approach to measuring fixed charge density in intervertebral disc tissue. *Ann Biomed Eng*. 2009;37(12):2566-2573.
38. Blake DA, McLean NV. A colorimetric assay for the measurement of D-glucose consumption by cultured cells. *Anal Biochem*. 1989;177(1):156-160.
39. Hulme CH, Westwood M, Myers JE, Heazell AEP. A high-throughput colorimetric-assay for monitoring glucose consumption by cultured trophoblast cells and placental tissue. *Placenta*. 2012;33(11):949-951.
40. Czamanski Salvatierra J, Yuan TY, Fernando H, et al. Difference in energy metabolism of annulus fibrosus and nucleus pulposus cells of the intervertebral disc. *Cell Mol Bioeng*. 2011;4(2):302-310.
41. Gantenbein B, Illien-Jünger S, Chan SCW, et al. Organ culture bioreactors—platforms to study human intervertebral disc degeneration and regenerative therapy. *Curr Stem Cell Res Ther*. 2015;10(4):339-352.
42. Chan SCW, Ferguson SJ, Gantenbein-Ritter B. The effects of dynamic loading on the intervertebral disc. *Eur Spine J*. 2011;20(11):1796-1812.
43. Illien-Jünger S, Gantenbein-Ritter B, Grad S, et al. The combined effects of limited nutrition and high-frequency loading on intervertebral discs with endplates. *Spine (Phila Pa 1976)*. 2010;35(19):1744-1752.
44. McGill University Health Centre, Rosenzweig DH, Gawri R, et al. Dynamic loading, matrix maintenance and cell injection therapy of human intervertebral discs cultured in a bioreactor. *Eur Cell Mater*. 2016;31:26-39.
45. Pfannkuche J, Guo W, Cui S, et al. Intervertebral disc organ culture for the investigation of disc pathology and regeneration—benefits, limitations, and future directions of bioreactors. *Connect Tissue Res*. 2019;61(3-4):304-321.
46. Wilke H-J, Neef P, Caimi M, Hoogland T, Claes LE. New in vivo measurements of pressures in the intervertebral disc in daily life. *Spine (Phila Pa 1976)*. 1999;24(8):755-762.
47. Buttermann GR, Beaubien BP, Saeger LC. Mature runt cow lumbar intradiscal pressures and motion segment biomechanics. *Spine J*. 2009;9(2):105-114.
48. Haglund L, Moir J, Beckman L, et al. Development of a bioreactor for axially loaded intervertebral disc organ culture. *Tissue Eng Part C Methods*. 2011;17(10):1011-1019.
49. Adams MA, McNally DS, Dolan P. “Stress” distributions inside intervertebral discs the effects of age and degeneration. *J Bone Jt Surg*. 1996;78(6):965-972.
50. McDonnell EE, Buckley CT. Consolidating and re-evaluating the human disc nutrient microenvironment. *JOR Spine*. 2022;e1192:1-20.
51. Wang D, Hartman R, Han C, et al. Lactate oxidative phosphorylation by annulus fibrosus cells: evidence for lactate-dependent metabolic symbiosis in intervertebral discs. *Arthritis Res Ther*. 2021;23(1):1-16.
52. Wang C, Gonzales S, Levene H, Gu W, Huang CYC. Energy metabolism of intervertebral disc under mechanical loading. *J Orthop Res*. 2013;31(11):1733-1738.
53. Neidlinger-Wilke C, Mietsch A, Rinkler C, Wilke HJ, Ignatius A, Urban J. Interactions of environmental conditions and mechanical loads have influence on matrix turnover by nucleus pulposus cells. *J Orthop Res*. 2011;30(1):112-121.
54. Wong J, Sampson SL, Bell-Briones H, et al. Nutrient supply and nucleus pulposus cell function: effects of the transport properties of the cartilage endplate and potential implications for intradiscal biologic therapy. *Osteoarthr Cartil*. 2019;27(6):956-964.
55. Shalash W, Ahrens SR, Bardanova LA, Byvaltsev VA, Giers MB. Patient-specific apparent diffusion maps used to model nutrient availability in degenerated intervertebral discs. *JOR Spine*. 2021;4(4):e1179.
56. Lama P, Claireaux H, Flower L, et al. Physical disruption of intervertebral disc promotes cell clustering and a degenerative phenotype. *Cell Death Dis*. 2019;5(154):1-9.
57. McDonnell EE, Buckley CT. Investigating the physiological relevance of ex vivo disc organ culture nutrient microenvironments using in silico modeling and experimental validation. *JOR Spine*. 2021;4(2):1-16.
58. Feng C, Zhang Y, Yang M, et al. Transcriptome and alternative splicing analysis of nucleus pulposus cells in response to high oxygen tension: involvement of high oxygen tension in the pathogenesis of intervertebral disc degeneration. *Int J Mol Med*. 2018;41(6):3422-3432.
59. Jähn K, Stoddart MJ. Viability assessment of osteocytes using histological lactate dehydrogenase activity staining on human cancellous bone sections. *Mammalian Cell Viability*. Humana Press; 2011:141-148.
60. Hu X, Chao M, Wu H. Central role of lactate and proton in cancer cell resistance to glucose deprivation and its clinical translation. *Signal Transduct Target Ther*. 2017;2(e16047):1-8.
61. Wu H, Ding Z, Hu D, et al. Central role of lactic acidosis in cancer cell resistance to glucose deprivation-induced cell death. *J Pathol*. 2012;227(2):189-199.
62. Loibl M, Wuertz-Kozak K, Vadala G, Lang S, Fairbank J, Urban JP. Controversies in regenerative medicine: should intervertebral disc degeneration be treated with mesenchymal stem cells? *JOR Spine*. 2019;2(1):e1043.
63. Williams RJ, Tryfonidou MA, Snuggs JW, Le Maitre CL. Cell sources proposed for nucleus pulposus regeneration. *JOR Spine*. 2021;4(4):1-27.
64. Naqvi SM, Buckley CT. Extracellular matrix production by nucleus pulposus and bone marrow stem cells in response to altered oxygen and glucose microenvironments. *J Anat*. 2015;227(6):757-766.
65. Gansau J, Buckley CT. Priming as a strategy to overcome detrimental PH effects on cells for intervertebral disc regeneration. *Eur Cell Mater*. 2021;41:153-169.
66. Schmitz TC, Salzer E, Crispim JF, et al. Characterization of biomaterials intended for use in the nucleus pulposus of degenerated intervertebral discs. *Acta Biomater*. 2020;114:1-15.

67. Bonnaire FC, Danalache M, Sigwart VA, Breuer W, Rolauffs B, Hofmann UK. The intervertebral disc from embryonic development to disc degeneration: insights into spatial cellular organization. *Spine J*. 2021;21(8):1387-1398.
68. Miyazaki T, Kobayashi S, Takeno K, Meir A, Urban J, Baba H. A phenotypic comparison of proteoglycan production of intervertebral disc cells isolated from rats, rabbits, and bovine tails; which animal model is most suitable to study tissue engineering and biological repair of human disc disorders? *Tissue Eng Part A*. 2009;15(12):3835-3846.
69. Sadowska A, Hausmann ON, Wuertz-Kozak K. Inflammaging in the intervertebral disc. *Clin Transl Neurosci*. 2018;20(1):48-59.

## SUPPORTING INFORMATION

Additional supporting information can be found online in the Supporting Information section at the end of this article.

**How to cite this article:** Salzer, E., Mouser, V. H. M., Bulsink, J. A., Tryfonidou, M. A., & Ito, K. (2023). Dynamic loading leads to increased metabolic activity and spatial redistribution of viable cell density in nucleus pulposus tissue. *JOR Spine*, 6(1), e1240. <https://doi.org/10.1002/jsp2.1240>